Available online at www.CivileJournal.org

Civil Engineering Journal

(E-ISSN: 2476-3055; ISSN: 2676-6957)

Vol. 7, No. 08, August, 2021

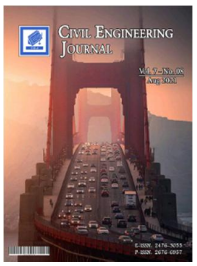

Strengths of Struts and Nodal Zones for Strut-and-Tie Model Design of Reinforced Concrete Corbels

Young Mook Yun [1*], Youjong Lee [2]

[1] Professor, Dept. of Civil Engineering, Kyungpook National University, South Korea.

[2] Graduate Student, Dept. of Civil Engineering, Kyungpook National University, Daegu 41566, South Korea.

Received 28 April 2021; Revised 07 July 2021; Accepted 17 July 2021; Published 01 August 2021

Abstract

The strut-and-tie model (STM) method is useful for the limit state design of reinforced concrete (RC) corbels. However, for the rational design of RC corbels, designers must accurately determine the strengths of concrete struts and nodal zones to check the strength conditions of a selected STM and the anchorage of reinforcing bars in nodal zones. In this study, the authors suggested a numerical process for determining the strengths of concrete struts and nodal zones in RC corbel STMs. The technique incorporates the state of two-dimensional (2-D) stresses at the strut and nodal zone locations, 2-D failure envelope of concrete, deviation angle between the strut orientation and compressive principal stress trajectory, and the effect of concrete confinement by reinforcing bars. The authors also proposed the strength equations of struts and nodal zones that apply to the typical determinate and indeterminate STMs of RC corbels. The authors considered the effects of the shear span-to-effective depth ratio, the horizontal-to-vertical load ratio, and the primary tensile and horizontal shear reinforcement ratios in developing the strength equations. The authors predicted the failure strengths of 391 RC corbels tested to examine the appropriateness of the proposed numerical process and strength equations. The predicted failure strength compares very well with experimental results, proving that the rational analysis and design of RC corbels are possible by using the present study's strut and nodal zone strengths.

Keywords: Reinforce Concrete Corbel; Strut-and-Tie Model; Concrete Strut; Nodal Zone.

1. Introduction

RC corbel is a representative structural member with static discontinuities due to the concentrated vertical and horizontal loads. The primary design codes, including FIB [1], AASHTO [2], ACI 318 [3], have accepted the STM method for the design of RC corbels. The STM method promotes a better understanding of the load transfer mechanism, thus improving a designer's ability to handle unusual design circumstances. However, to employ the method in practice, a structural designer must determine the strengths of struts and nodal zones to verify their load-carrying capacities.

Many researchers have conducted experimental and analytical studies on the strength of concrete struts and nodal zones. The readers can find various suggested strength equations and values from previous researches [1-15]. However, the suggested equations and values are not consistent and general because they base on structural concretes with specific loading and geometric conditions. Yun & Ramirez [16] proposed a numerical method for determining

* Corresponding author: ymyun@knu.ac.kr

http://dx.doi.org/10.28991/cej-2021-03091725

the strut strengths in three-dimensional (3-D) structural concrete. The method accurately determines the stress levels of concrete struts for 3-D STM design situations. However, it is inefficient to implement in practice since the method requires very complicated numerical calculations and iterative 3-D finite element linear analyses of unreinforced concrete members and selected STMs. Therefore, strength values of concrete struts and nodal zones applicable to all general cases must be provided for the rational STM design of structural concrete.

In this study, the authors presented a numerical process for determining the strengths of concrete struts and nodal zones in RC corbels. The approach considers the state of 2-D principal stresses at the strut and nodal zone locations, 2-D failure envelope of concrete, deviation angle between the directions of the concrete strut and principal compressive stress, and the effect of concrete confinement by reinforcing bars. The process requires numerical calculations and iterative linear elastic finite element analyses of disturbed regions and selected STMs. Thus, for use in practice, the authors developed the strength equations of concrete struts and nodal zones for previous studies' typical corbel STMs. The authors examined the validity of strength equations by predicting 391 RC corbels' failure strengths with the typical STMs.

In Section 2 of this paper, the authors introduced three types of statically determinate and indeterminate corbel STMs that designers employ in practice. In addition, the authors introduced the strength equations/values of struts and nodal zones suggested by the current design codes and the present study. In Section 3, the authors predicted the failure strengths of RC corbels by using three types of corbel STMs to evaluate the properness of the existing and proposed strength values of concrete struts and nodal zones. The authors provided a detailed STM procedure for estimating the failure strength of corbels with tables and figures. In Section 4, the authors concluded the research results of this paper.

2. STM and Strength of Struts and Nodal Zones

2.1. Strut-and-Tie Model

Although the current design codes stipulate the use of the STM method for the limit state design of a corbel, they do not recommend STMs for RC corbels specifically. Three types of simple determinate and indeterminate STMs are general for corbel analysis and design. Most books and publications dealing with disturbed regions, including Bergmeister et al. [10], ACI 445 [17], Collins & Mitchel [20], Nawy [21], and Wight [22] introduced a determinate STM representing an arch mechanism, as shown in Figure 1(a). The arch mechanism transfers an external load to a column directly by an inclined concrete strut. KCI [19] introduced a determinate STM representing a truss mechanism, shown in Figure 1(b). The truss mechanism transfers an external load to a column by inclined concrete struts and a horizontal steel tie. Chae & Yun [18] proposed a first-order statically indeterminate STM for RC corbels. The proposed model, defined as a combined mechanism, is shown in Figure 1(c). As the axial forces in the indeterminate STM depend on the struts and ties' axial stiffness, they suggested a load distribution ratio that transforms the indeterminate STM into a determinate one:

$$\alpha(\%) = \frac{F_E}{P} \times 100 = A(a/d - B)^2 + C \tag{1}$$

where the parameters A, B, and C are functions of the shear span-to-effective depth ratio, the compressive strength of the concrete, the primary tensile reinforcement ratio, the minimum flexural reinforcement, and the horizontal-to-vertical load ratio. Details of parameters are described in the reference.

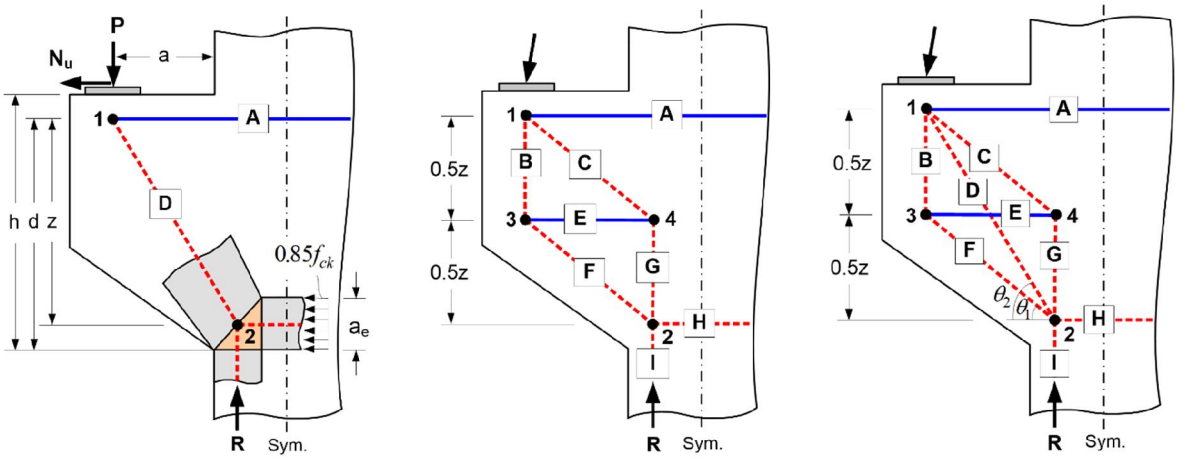

(a) (b) (c)

Figure 1. STMs for RC Corbels. (a) Arch Mechanism. (b) Truss Mechanism. (c) Combined Mechanism

2.2. Strength Equations of Design Codes

EC2 [13] proposed the following strength equation for struts and nodal zones:

$$f_c = \nu_1 \nu_2 f_{cd} \tag{2}$$

where f_{cd} is the design value of the cylinder strength of concrete f'_c in MPa. f_{cd} equals $\alpha_{cc} f_{ck}/\gamma_c$, where f_{ck} is the characteristic value of the cylinder strength of concrete in MPa, α_{cc} (=0.85~1.0) is the coefficient accounting for long term effects on the compressive strength, and γ_c (=1.5) is the partial safety factor for the concrete. ν_1 is 1.0 for the strut in a uniaxial compression stress state and for the nodal zone bounded by struts, bearing area, or both (CCC-nodal zone), 0.85 for the nodal zone anchoring one tie (CCT-nodal zone), 0.6 for the for the strut subjected to tensile stresses transverse to the strut, and 0.75 for the nodal zone anchoring two or more ties (CTT-nodal zone). ν_2 is 1.0 for the strut in a uniaxial compression stress state, $1 - f_{ck}/250$ for the strut subjected to tensile stresses transverse to the strut and for all nodal zones.

FIB [1] also proposed Equation 2, where ν_1 is 1.0 for the strut in undisturbed uniaxial compression stress states, for the strut in regions with transverse compression, and for CCT-nodal zone. Besides, ν_1 is 0.75 for the strut with cracks parallel to the direction of compression and tension reinforcement perpendicular to this and for CCT- and CTT-nodal zone, and 0.55 for the strut with reinforcement running obliquely. ν_2 equals $(30/f_{ck})^{1/3}$. The code limits the value of $\nu_1 \nu_2$ to 1.0, 0.8, and 0.55 for the three cases of struts, as mentioned above, and 1.0 for all nodal zones. DIN [15] proposed Equation 2, too, where ν_1 is 1.0 for the strut in uncracked compressive zones and CCC-nodal zone and 0.75 for the strut with cracks parallel to the direction of compression and CCT- and CTT-nodal zone. ν_2 equals $0.4 + 0.6(0.16 f_{ctm}/(2200 f_{yk}))$ for lightweight concrete and 1.0 for normal weight concrete, where f_{ctm} and f_{yk} are the mean values of the axial tensile strength of concrete and the characteristic tensile strength of the reinforcement. CSA [14] proposed the equation for the strength of concrete struts as follows:

$$f_c = \frac{f_c^{'}}{0.80 + 170(\varepsilon_s + (\varepsilon_s + 0.002)\cot^2 a_s)} \tag{3}$$

Where ε_S and a_s are the tensile strain of a steel tie crossing a concrete strut and the smallest angle between the steel tie and the concrete strut, respectively. The codes suggested $0.85\beta_c f_{ck}$, $0.75\beta_c f_{ck}$, and $0.65\beta_c f_{ck}$ as the strengths of CCC-, CCT-, and CTT-nodal zone, respectively. Here, β_c equals lesser of 2.0 and $\sqrt{A_2/A_1}$ (A_1= area under the bearing device, A_2= area of the lower base of the largest frustum of a pyramid, cone, or tapered wedge contained wholly within the support and having its upper base equal to the loaded area) if a bearing or loading plate connects to the nodal zone. β_c is zero if a bearing or loading plate does not connect to the nodal zone.

Lately, ACI 318 [3] proposed the equation for the strength of concrete struts and nodal zones by considering the shape of a concrete strut, the amount of reinforcement confining the strut, and the influence of concrete confinement effect as follows:

$$f_c = 0.85\beta_c \beta_s f_c^{'} \tag{4}$$

where β_c is a strut confinement modification factor. β_c is lesser of $\sqrt{A_2/A_1}$ and 2.0 for strut whose end of a strut connected to a node that includes a bearing surface. β_s is a factor that accounts for the effects of cracks and confining reinforcement. Detailed explanations, values, and related equations about β_s for strut strength are given in the reference. β_s is 1.0, 0.8, and 0.6 for CCC-, CCT-, and CTT-nodal zone, respectively.

2.3. Strength of Present Study

In the present study, the authors introduce a numerical method to determine 2-D concrete struts and nodal zones' strength levels. The procedure of the method is as follows.

Stage 1: After constructing a finite element model for a concrete member's disturbed region, determine the principal stresses (σ_{1p} and σ_{2p}) and principal angles of the finite elements by conducting a linear elastic finite element analysis. Then, construct an STM that describes a proper load transfer mechanism of the region by considering the principal stress trajectories and patterns of reinforcement. Lastly, collect the finite elements close to the centreline of each concrete strut.

Stage 2: Determine the principal failure strengths of each collected finite element, σ_{1f} and σ_{2f} ($\geq \sigma_{1f}$), by extending a line connecting the points (0, 0) and (σ_{1p}, σ_{2p}) to the failure envelope straightly. Here, σ_{1f} obtained from the failure envelope corresponds to f_{cs}^e, the principal failure strength of a finite element acting toward the concrete strut's longitudinal direction.

Stage 3: Calculate the deviation angle θ between the directions of the concrete strut and the principal compressive stress of the finite element to adjust the principal failure strength f_{cs}^e as follows:

$$\begin{bmatrix} f_{11}(=f_{cs}^{e}) & f_{12} \\ f_{21} & f_{22} \end{bmatrix} = \begin{bmatrix} \cos\theta & \sin\theta \\ -\sin\theta & \cos\theta \end{bmatrix} \begin{bmatrix} \sigma_{1f} & 0 \\ 0 & \sigma_{2f} \end{bmatrix} \begin{bmatrix} \cos\theta & \sin\theta \\ -\sin\theta & \cos\theta \end{bmatrix}^{T} \quad (5)$$

Then, obtain the concrete strut's strength by averaging the principal failure strengths of the finite elements (that located near along the longitudinal axis of the strut) in the standard deviation range. The reason for taking the average in the standard deviation range is to minimize the effect of the variation of the stresses of the finite elements placed along the strut's longitudinal axis. The nodal zone's strength in the direction of the strut's longitudinal axis equals the average of the principal failure strengths of the finite elements located at the nodal zone area.

Stage 4: Conduct a structural analysis of the STM using concrete struts' strengths determined in Stage 3. Then, along with the external forces, apply the steel ties' axial forces to the finite element model of the disturbed region and iterate the procedure from Stage 1. This iteration continues until the difference between the newly and previously determined axial forces of the steel ties reaches a tolerance limit. Figure 2 shows the iterative procedure for considering the confinement effect by reinforcing bars.

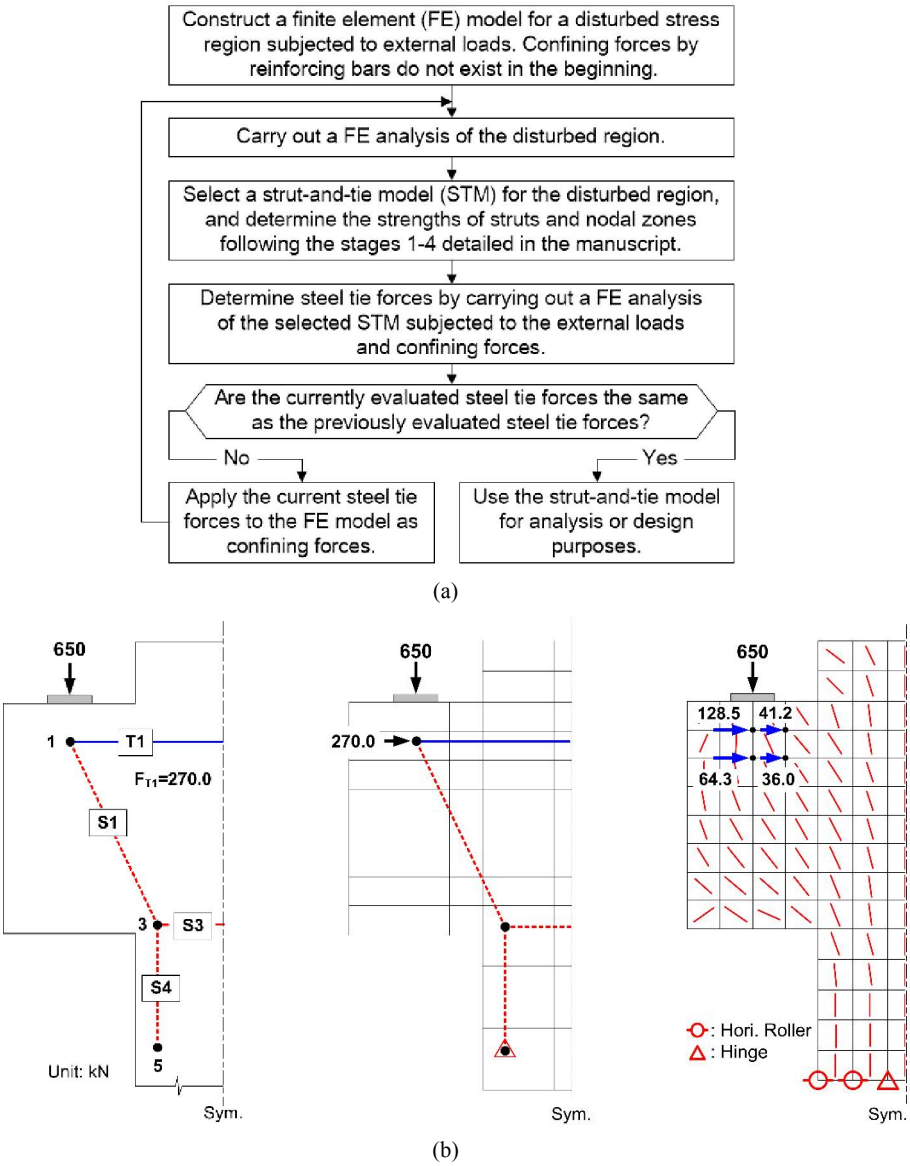

Figure 2. Algorithm for Considering Confinement Effect of Concrete by Reinforcing Bars. (a) Algorithm. (b) Example

The procedure mentioned above requires considerable effort and iterative finite element analyses of the unreinforced concrete member and STM. Thus, the authors determined the strengths of concrete struts for the three types of corbel STMs shown in Figure 1 using the above procedure, considering numerous combinations of design variables. By using a curve-fitting process, the authors developed the strength coefficient of the concrete strut, $\nu_s(=f_c/f_c')$, as follows:

$$v_s = \alpha_1 \rho_s \rho_h + \alpha_2 \rho_s + \alpha_3 \rho_h + \alpha_4 \quad (6)$$

where ρ_s is the tensile reinforcement ratio defined by $A_{s\,prov}/A_{s\,req'd}$, ρ_h is the horizontal shear reinforcement ratio defined by $A_{h\,prov}/A_{h\,req'd}$, and a/d is the shear span-to-effective depth ratio of the corbel. Here, $A_{s\,prov}$ and $A_{h\,prov}$ are the areas of the primary tensile and horizontal shear reinforcing bars that will be (or were) placed be in a corbel, respectively. $A_{s\,req'd}$ (= $(P \times a/Z + N_u)/f_y$, $z = 0.9d$, and f_y is the yield strength of the steel) and $A_{h\,req'd}$ (=$(P \times a/Z)/f_y$) are the areas of the primary tensile and horizontal shear reinforcing bars that resist the external vertical force *P*and horizontal force N_u. The strength coefficient is valid for the corbels with ranges of $0.4 \le \rho_s \le 1.0$, $0 \le \rho_h \le 1.0$, and $a/d \le 1.40$. The parameters α_i ($i = 1 \sim 4$) for the strength coefficient of strut *D* are as follows:

$$\begin{cases} \alpha_1 = -0.7(a/d)^2 + 1.2(a/d) - 0.5 \\ \alpha_2 = -0.7(a/d)^2 + 1.3(a/d) \\ \alpha_3 = 0.6(a/d)^2 - 1.2(a/d) + 0.6 \\ \alpha_4 = 0.8(a/d)^2 - 1.4(a/d) + 1.0 \end{cases} \quad (7)$$

Figure 3 shows the strength coefficients v_s and the parameter α_i for struts B, C, F, and G. Using the same procedure, the authors also determined the strength of the nodal zone at node 1 (nodal zone 1) of the corbel STMs showed in Figure 1. By using a curve-fitting process, the authors developed the strength coefficient of nodal zone 1, $v_n (= f_c / f_c)$, in the directions of struts *B*, *C*, and *D* as follows:

$$\begin{cases} v_n = (-1.7N_u/P + 0.3)(a/d) + 0.6N_u/P + 1 & for \quad a/d \le 0.3 \\ v_n = -0.8(a/d) + 1.3 & for \quad 0.3 < a/d \le 1.4 \end{cases} \quad (8a)$$

$$\begin{cases} v_n = (-N_u/P + 0.3)(a/d) + 0.5N_u/P + 0.9 & for \quad a/d \le 0.3 \\ v_n = 1.3 & for \quad 0.3 < a/d \le 1.4 \end{cases} \quad (8b)$$

$$\begin{cases} v_n = (-0.2N_u/P + 0.1)(a/d) + 0.4N_u/P + 1 & for \quad a/d \le 0.3 \\ v_n = -0.1(a/d) + 1.1 & for \quad 0.3 < a/d \le 1.4 \end{cases} \quad (8c)$$

In Equation 8, the maximum value of N_u/P is limited to 0.20. The nodal zone at node 2 (nodal zone 2) of the corbel is the CCC-node confined by all the struts framing into the node. Thus, the authors recommend 0.95 for the strength coefficient.

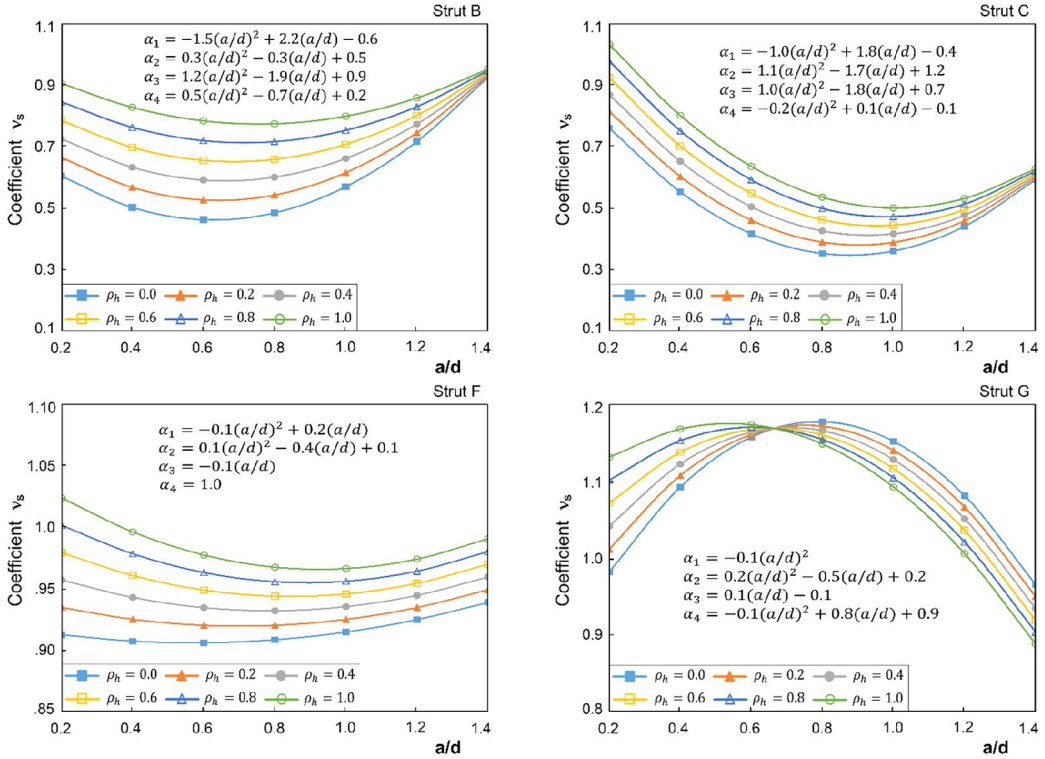

Figure 3. Strength Coefficients of Concrete Struts ($\rho_s = 1.0, N_u/P = 0.2$)

3. Verifications

Using the three types of STMs shown in Figure 1, the authors predicted 380 RC corbels' failure strengths to examine the properness of the existing and proposed strength values of concrete struts and nodal zones. The corbels were tested by Kriz & Raths [23], Hermansen & Cowan [24], Mattock et al. [25], Fattuhi & Hughes [26, 27], Yong & Balaguru [28], Fattuhi [29-31], Foster et al. [32], Bourget et al. [33], Campione et al. [34, 35], Yang et al. [36], Urban & Krawczyk [37], Khosravikia et al. [38], Wilson et al. [39], Abdul-Razzaq & Dawood [40], Ivanova et al. [41], Abdulridha et al. [42], Romanichen and Souza [43], Al-Talqany and Alhussainy [44], and Shakir [45]. Table 1 shows the specifications and ranges of the primary design variables of the corbels. The references above provide the test setups, rebar details, failure patterns, and additional details.

3.1. Strength Prediction Using Determinate STMs

The authors used corbel PG2, one of the corbels tested by Foster et al. [32], to illustrate the procedure for predicting the corbel's failure strength by using determinate STMs. Figure 4 shows the geometrical shape and reinforcement details of the corbel. The shear span-to-effective depth ratio a/d, the

Table 1. Details of RC Corbels tested to Failure.

Investigators	No. of Corbels	b (mm)	c (mm)	d (mm)	h (mm)	f'_c (MPa)	f_y (MPa)	a/d	ρ/ρ_{min}
Kriz & Raths [23]	185	203-406	152-610	307-1059	457-660	16.9-42.2	293-498	0.11-0.62	0.601-6.675
Hermansen & Cowan [24]	40	152-228	152-381	119-375	254-406	17.6-49.2	317-359.3	0.29-1.01	1.120-14.165
Mattock et al. [25]	28	152	152-330	221-231	254	23.8-30.7	321-447	0.22-1.02	2.956-9.615
Fattuhi & Hughes [26, 27]	21	150-152	150-152	103-135	148-150	32.2-57.4	491-558	0.44-1.04	1.801-4.145
Fattuhi [29-31]	28	150-154	150-152	92-226	150-251	24.6-70.7	427-454	0.44-1.46	1.110-11.459
Yong & Balaguru [28]	14	254	356	305	406	39.2-79.5	420	0.25-0.75	0.902-3.154
Foster et al. [32]	30	125-150	300-550	450-740	600-800	45.0-105	415-495	0.30-1.00	0.678-8.189
Bourget et al. [33]	7	150	300	321-338	360	70-132	525-550	0.25-0.38	0.652-1.642
Campione et al. [34, 35]	12	160	160	130-140	140-160	48.5-79	488-570	0.84-1	1.191-3.534
Yang et al. [36]	2	160	160	303	350	83.8	499	0.33	2.656
Urban & Krawczyk [37]	3	200	200	225-284	245-300	23.9-35	409-628	0.52-0.66	1.519-4.133
Khosravikia et al. [38]	3	355	355	572	610	29.4	471-570	0.58	3.054-4.165
Wilson et al. [39]	4	355.6	355.6	558.8	610	36-47.1	487-506	0.59-0.65	2.966-4.130
Abdul-Razzaq & Dawood [40]	3	115	250	350	390	33.0-33.7	450	0.5-1.5	5.076-5.183
Ivanova et al. [41]	1	150	300	340	360	30.0	585	0.45	1.697
Abdulridha et al. [42]	2	150	200	200	250	28.0-57.0	401	0.84	2.104-4.214
Romanichen & Souza [43]	2	200	250	350	400	25.0	493	0.60-1.00	5.774
Al-Talqany & Alhussainy [44]	4	150	150	127.5	150	80.5	493	0.50-1.00	1.885-2.312
Shakir [45]	2	200	200	220	250	57.1	510	0.70-1.00	3.400
Total	391	115-406	150-610	92-1059	148-800	16.9-132	293-628	0.11-1.5	0.601-14.165

b, c, d, h: width, overhanging length, effective depth, height of corbel; f'_c: compressive strength of concrete; f_y: yield strength of steel; a/d: shear span-to-effective depth ratio; ρ: flexural reinforcement ratio; ρ_{min}: minimum flexural reinforcement ratio

Primary tensile reinforcement ratio ρ/ρ_{min}, the compressive strength of the concrete f'_c, the yield strengths of the primary tensile and horizontal shear reinforcing bars f_y, and the width of loading plate are 0.60, 2.94, 94.0 MPa, 415 and 490 MPa, and 100 mm, respectively.

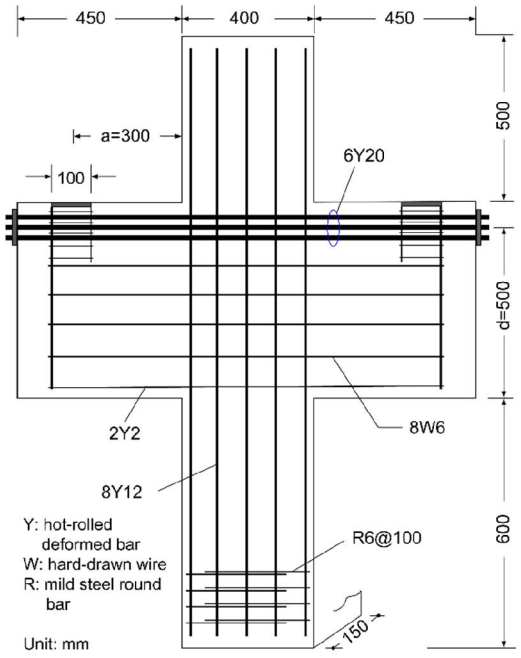

Figure 4. Rebar Details of Corbel PG2

Figures 5(a) and (b) show the determinate STMs for corbel PG2. In the models, the authors placed steel ties A and E at the centroid of the primary tensile and horizontal shear reinforcing bars. The authors located the horizontal concrete struts crossing the column to fit their widths' lower boundary lines to the bottom end of the corbel. The widths of the horizontal concrete struts are the same as the equivalent rectangular stress block's depth defined as $A_s f_y/(0.85 f_c' b)$ (A_s is the primary tensile reinforcement area and b=150 mm). The location of the vertical concrete strut placed at the column is dependent on the horizontal coordinate of node 2. In this study, as the failure strength changes according to the horizontal coordinate of node 2, the authors considered three different cases of horizontal coordinates of node 2.

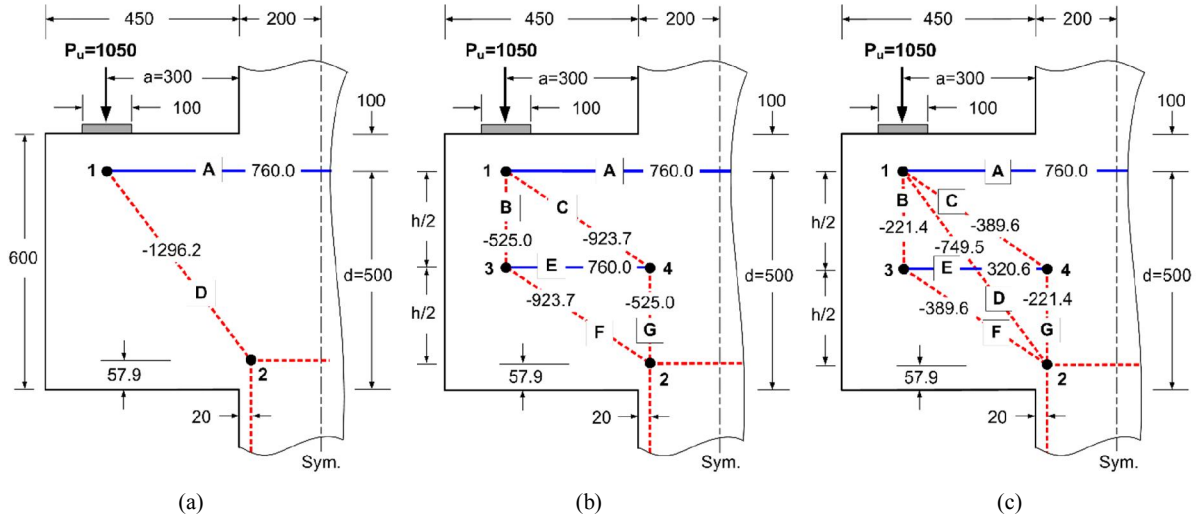

Figure 5. STMs for Corbel PG2. (a) Arch Mechanism. (b) Truss Mechanism. (c) Combined Mechanism

The authors determined the failure strength of corbel PG2 by using the STM methods of current design codes, requiring the verification of STM elements' load-carrying capacities, including concrete struts, steel ties, and nodal zones. The authors examined the load-carrying capacity by comparing the element's available area with its required area. The available areas of concrete struts and the nodal zone boundaries were determined by the ACI-ASCE 445 approach [46], which considers the STM's geometric shape and the loading and bearing plates' sizes. The steel tie's available area is the same as the area of reinforcing bars placed within the effective width of a steel tie. Figure 6 shows the available widths (areas) of the struts and ties of the determinate STMs. For cases in which two or three struts share one boundary of the nodal zone shown in Figures 6(b) and (c), the authors used the KCI [19] procedure (illustrated in

Figure 6(d) for a nodal zone under a loading plate) to determine the available widths of the struts. The authors obtained the required areas of the struts and ties under an experimental failure load by dividing the axial forces (shown in Figure 5) by their strengths. The authors also determined the required areas at the boundaries of a nodal zone by dividing the axial forces of the struts and ties framing the nodal zone by the nodal zone's strength.

The authors accounted for the tension-stiffening effect in the strength predictions by increasing the available area of horizontal steel tie A to the following amount:

$$A_{tie,add} = A_{tie,c} f_{TS} / f_y \tag{9}$$

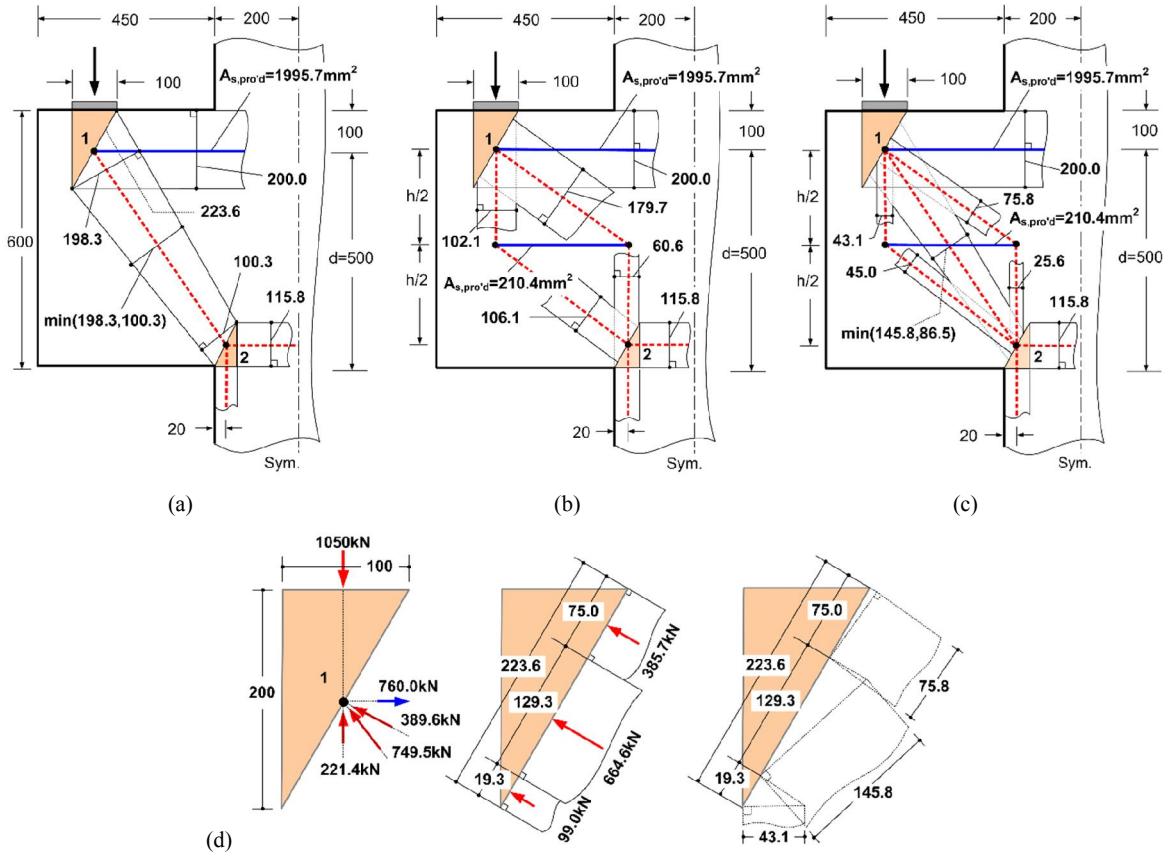

Figure 6. Available Widths of Concrete Struts and Nodal Zones in Corbel PG2 STMs. (a) Arch Mechanism. (b) Truss Mechanism. (c) Combined Mechanism. (d) Available Strut Widths at Node 1 of Combined Mechanism.

where $A_{tie,c}$ is the cross-sectional area of concrete at the location of steel tie A, f_y is the yield strength of the reinforcing bars in the tie, and f_{TS} is the concrete tensile stress suggested by Lee *et al*. [47]:

$$f_{TS} = (-0.0313\rho_s^{0.57} d_b + 3.3881\rho_s^{0.76})\sqrt{f_c'} \tag{10}$$

In Equation 10, ρ_s and d_b are the reinforcement ratio and the tie's rebar diameter, respectively.

Table 2 illustrates a detailed procedure for predicting the failure strength of corbel PG2 with the arch mechanism STM, proposed strut strengths, and Bergmeister et al.'s [10] nodal zone strength. As shown in the table, concrete strut D failed at a load of 888.3 kN (84.6% of the experimental failure load), and nodal zone 1 did not fail at this load. Thus, 84.6% of the failure load proved to be its failure strength. The nodal zone 2 did not fail in all corbels in tests; therefore, the authors did not verify the strength of nodal zone 2. The authors predicted the corbels' failure strengths with variable horizontal coordinates of node 2 using different strength values of concrete struts and nodal zone 1.

Table 3 lists the strength analysis results estimated by using determinate arch and truss corbel STMs. The average ratios of the calculated strength to experimental strength (and COV) by the determinate arch mechanism STM with the strut and nodal zone strengths of EC2, DIN, FIB, CSA, ACI 318, and the present study are 0.77 (34.9%), 0.81 (31.9%), 0.66 (28.5%), 0.87 (31.2%), 0.74(39.7%), and 0.97 (28.3%), respectively. The predicted failure strengths of 391 corbels are reasonably well on average by the determinate arch mechanism STM with the proposed strut and nodal zone strengths.

Table 2. Failure Strength Estimation of Corbel PG2 by Determinate Arch Mechanism STM

(a) Failure Strength Verification of Strut and Tie

Strut No.	ν_s	f'_c (MPa)	f_{cs} (MPa)	F_u (kN)	$w_{req'd}$ (mm)	$w_{pro'd}$ (mm)	$w_{pro'd}/w_{req'd}$	Safety
D	0.78	94.0	72.9	1296.2	118.6	100.3	**0.846**	×
Tie No.	ν_t	f_y (MPa)	f_{st} (MPa)	F_u (kN)	$A_{req'd}$ (mm^2)	$A_{pro'd}$ (mm^2)	$A_{pro'd}/A_{req'd}$	**Safety**
A	1.00	415.0	415	760.0	1831.3	1995.7	1.090	○

ν_s and ν_t: coefficients of strengths of strut and tie; strength of concrete strut $f_{cs} = \nu_s f'_c$; strength of steel tie $f_{st} = \nu_t f_y$; F_u: axial force under experimental failure load of 1050kN; $w_{req'd} = F_u/(bf_{cs})$; $w_{pro'd}$: available width of concrete strut (refer to Figure 6(a))

(b) Failure Strength Verification of Nodal Zone

Node No.	Node Type	ν_e	A, A_b (mm^2)	ν_n	f'_c (MPa)	f_{cn} (MPa)	F_u (kN)		$w_{req'd}$ (mm)	$w_{pro'd}$ (mm)	$w_{pro'd}/w_{req'd}$	Safety
1	CCT	0.65	500 × 150, 100 × 150	1.30	94.0	122.2	P	888.2	48.5	100.0	2.064	○
							Strut D	1096.4	49.0	223.6	4.566	○
							Tie A	642.8	35.1	200.0	5.703	○

$\nu_n (= \nu_e\sqrt{A/A_b}, A/A_b \le 4, \nu_e = 0.8$ for $f'_c \ge 70)$: coefficient of strength of nodal zone by Bergmeister et al. [10]; strength of nodal zone $f_{cn} = \nu_n f'_c$; F_u: axial force at nodal zone boundary under 84.6% of experimental failure load; P: applied load (=84.6% of experimental failure load); $w_{pro'd}$: available width of nodal zone boundary (refer to Figure 6(a))

Table 3. Failure Strength Estimated by Determinate Corbel STMs

(a) Arch Mechanism STM

P_{cal} / P_{test}

STM Model \ Strut & Node Strength	EC2 [13]	DIN [15]	FIB [1]	CSA [14]	ACI 318 [3]	Present Study
Model (A)	0.65	0.76	0.57	0.82	0.69	0.90
Model (B)	0.77	0.83	0.68	0.89	0.76	1.00
Model (C)	0.80	0.83	0.71	0.89	0.77	1.00
Mean (391)*	0.77	0.81	0.65	0.87	0.74	0.97
COV (%)	34.9	31.9	37.9	31.2	39.7	28.3

(A)~(C): STMs whose horizontal coordinates of node 2 are located at distances of 10, 15, and 20% of column width from the left face of the column, respectively; COV: coefficient of variation; ( )*: number of corbels.

(b) Truss Mechanism STM

P_{cal} / P_{test}

STM Model \ Strut & Node Strength	EC2 [13]	DIN [15]	FIB [1]	CSA [14]	ACI 318 [3]	Present Study
Model (A)	0.68	0.77	0.58	0.64	0.63	0.82
Model (B)	0.76	0.83	0.66	0.73	0.69	0.98
Model (C)	0.78	0.82	0.69	0.73	0.72	1.01
Mean (146)*	0.74	0.81	0.64	0.70	0.68	0.94
COV (%)	33.5	32.0	36.8	39.0	34.5	29.6

( )*: number of corbels having horizontal shear reinforcing bar(s); Yielding of steel ties describing horizontal shear reinforcing bars is prevented.

The authors speculate that the more conservative results by the design codes come from using the improper (lower) strengths of struts and nodal zones. The average strength coefficients of the inclined strut (and CCT nodal zone) in the arch mechanism STM by EC2, DIN, FIB, CSA, and ACI 318 are 0.51(0.72), 0.64(0.64), 0.44(0.61), 0.76(0.76), and 0.56(0.69), respectively. Whereas the average strength coefficient by the present study is 0.85(1.03). The differences in the strength coefficients between the design codes and the present study are mainly due to the different ways of considering the confinement effects by reinforcing bars. Besides, the expected failure strengths of 146 corbels (with horizontal shear reinforcing bars) are reasonably well by the truss mechanism STM with the proposed strengths. The same inference about the strength analysis results applies to the truss mechanism STM. The average strength coefficients of the inclined struts B, C, F, and G (and CCT nodal zone) in the truss mechanism STM in Figure 5(b) by EC2, DIN, FIB, CSA, ACI 318, and the present study are 0.51(0.72), 0.64(0.64), 0.44(0.61), 0.54-0.85(0.76), 0.46-0.58(0.69), and 0.59-1.11(0.91-1.05), respectively. These outcomes imply that the proposed strut and nodal zone strengths are appropriate for analyzing and designing a corbel with the determinate STMs.

3.2. Strength Prediction Using Indeterminate STM

By using the indeterminate STM shown in Figure 1(c), the authors examined the failure strengths of the corbels tested to failure. The same corbel, PG2, was used to illustrate the strength evaluation procedure. Figure 5(c) shows the selected indeterminate STM for corbel PB2. The authors located the steel ties A and E at the centroid of the primary tensile and horizontal shear reinforcing bars. The authors placed the horizontal concrete strut crossing the column to fit the lower boundary line of its width to the corbel's bottom end. The width of the horizontal concrete strut equals the depth of an equivalent rectangular stress block. As the failure strength changes according to the horizontal coordinate of node 2, the authors considered three different cases of horizontal coordinates of node 2, as in the determinate STMs.

The authors determined the failure strength of corbel PG2 by verifying the load-carrying capacities of STM elements, including concrete struts, steel ties, and nodal zones. The authors examined the load-carrying abilities by comparing the elements' available areas with their required areas. The authors obtained the available areas using the ACI-ASCE 445 approach [46], as in the determinate STMs. The authors considered the tension-stiffening effect at the location of steel tie A. Figure 6(c) shows the available widths (areas) of the struts and ties. The required areas of the struts and ties were obtained by dividing the axial forces shown in Figure 5(c) by their strengths. The authors calculated the elements' axial forces using the equilibrium equations at the nodes of determinate STM. Since the STM is an indeterminate truss structure, the authors used the load distribution ratio α (%), defined in Equation 1, to transform the indeterminate truss structure into a determinate structure.

Table 4 and Figure 7 explain a detailed procedure for evaluating the failure strength of corbel PG2 by using the indeterminate STM with the proposed strut strengths and Bergmeister et al.'s [10] nodal zone strength. Since the indeterminate STM reflects both the arch and truss load transfer mechanisms simultaneously, the authors determined the failure strength of the corbel following the sequential failure of both load transfer mechanisms. As illustrated in Table 4(a) and Figure 7(a), the first failure of the indeterminate STM occurred by the steel tie E's yielding at a load of 289.5 kN (27.6% of the experimental failure load). After the first failure, the indeterminate STM became determinate arch mechanism STM one, as shown in Figure 7(b). The arch mechanism STM could still transfer a fraction of the applied load to the column by steel tie A and inclined strut D. The authors added the remaining areas of struts B and C to the area of strut D at the boundary of nodal zone 1. As shown in Table 4(b) and Figure 7(c), the second failure of the STM occurred due to strut D's failure under an additional load of 709.7 kN (67.6% of the experimental failure load). After the second failure, the STM became an unstable truss structure that could not carry any additional load, as shown in Figure 7(d). At 999.2 kN (289.5+709.7 kN, 95.2% of the experimental failure load), which the indeterminate STM could carry to the utmost limit by the concrete struts and steel ties, the authors examined the strength of the nodal zone 1, as illustrated in Table 4(c) and Figure 7(e). Since nodal zone 1 did not fail, 95.2% of the experimental failure load becomes the corbel's failure strength. Since the nodal zones 2, 3, and 4 did not fail in all corbel tests, the authors did not verify those nodal zones' failure. Similarly, the authors predicted the corbels' failure strengths with variable horizontal coordinates of node 2 by using different strength values of concrete struts and nodal zone 1.

Table 4. Failure Strength Estimation of Corbel PG2 by an Indeterminate STM

(a) Failure Strength Verification of Struts and Ties at the First State

Strut No.	ν_s	f'_c (MPa)	f_{cs} (MPa)	F_u (kN)	$w_{req'd}$ (mm)	$w_{pro'd}$ (mm)	$w_{pro'd}/w_{req'd}$	**Safety**
B	0.48	94.0	45.6	221.4	32.4	43.1	1.330	○
C	0.62	94.0	58.1	389.6	44.7	75.8	1.695	○
D	0.79	94.0	74.0	749.5	67.5	86.5	1.281	○
F	0.81	94.0	75.9	389.6	34.2	45.0	1.314	○
G	0.81	94.0	75.9	221.4	19.4	25.6	1.314	○
Tie No.	ν_t	f_y (MPa)	f_{st} (MPa)	F_u (kN)	$A_{req'd}$ (mm^2)	$A_{pro'd}$ (mm^2)	$A_{pro'd}/A_{req'd}$	**Safety**
A	1.00	415.0	415.0	760.0	1831.3	1995.7	1.090	○
E	1.00	420.0	420.0	320.6	763.2	210.4	0.276	×

ν_s and ν_t: coefficients of strengths of strut and tie; strength of concrete strut $f_{cs} = \nu_s f'_c$; strength of steel tie $f_{st} = \nu_t f_y$; F_u: axial force under experimental failure load of 1050kN; $w_{req'd} = F_u/(bf_{cs})$; $w_{pro'd}$: available width of concrete strut (refer to Figure 6(c)).

(b) Failure Strength Verification of Strut and Tie at the Second State

Strut No.	ν_s	f'_c (MPa)	f_{cs} (MPa)	F_u (kN)	$w_{req'd}$ (mm)	$w_{pro'd}$ (mm)	$w_{pro'd}/w_{req'd}$	Safety
D	0.79	94.0	74.0	1296.2	116.8	78.9	**0.676**	×
Tie No.	ν_t	f_y (MPa)	f_{st} (MPa)	F_u (kN)	$A_{req'd}$ (mm^2)	$A_{pro'd}$ (mm^2)	$A_{pro'd}/A_{req'd}$	Safety
A	1.00	415.0	415.0	760.0	1831.3	1490.8	0.814	×

F_u: axial force under experimental failure load of 1050kN; $w_{pro'd}$: available width of concrete strut after the first failure (refer to Figure 7(b)).

(c) Failure Strength Verification of Nodal Zone

Node No.	Node Type	v_e	A, A_b (mm^2)	v_n	f'_c (MPa)	f_{cn} (MPa)	F_u (kN)		$w_{req'd}$ (mm)	$w_{pro'd}$ (mm)	$w_{pro'd}/w_{req'd}$	Safety
							P	999.2				
							Strut B	61.0				
1	CCT	0.65	500×150, 100×150	1.30	94.0	122.2	Strut C	107.4	55.1	223.6	4.059	O
							Strut D	1082.7				
							Tie A	723.2	39.5	200.0	5.069	O

$v_n(=v_e\sqrt{A/A_b},\ A/A_b \le 4,\ v_e = 0.8$ for $f'_c \ge 70)$: coefficient of strength of nodal zone by Bergmeister et al. [10]; strength of nodal zone $f_{cn} = v_n f'_c$; F_u: axial force under 95.2%(=27.6+67.6) of experimental failure load; P: applied load (=95.2% of experimental failure load); $w_{pro'd}$: available width of nodal zone boundary (refer to Figure 7(e)).

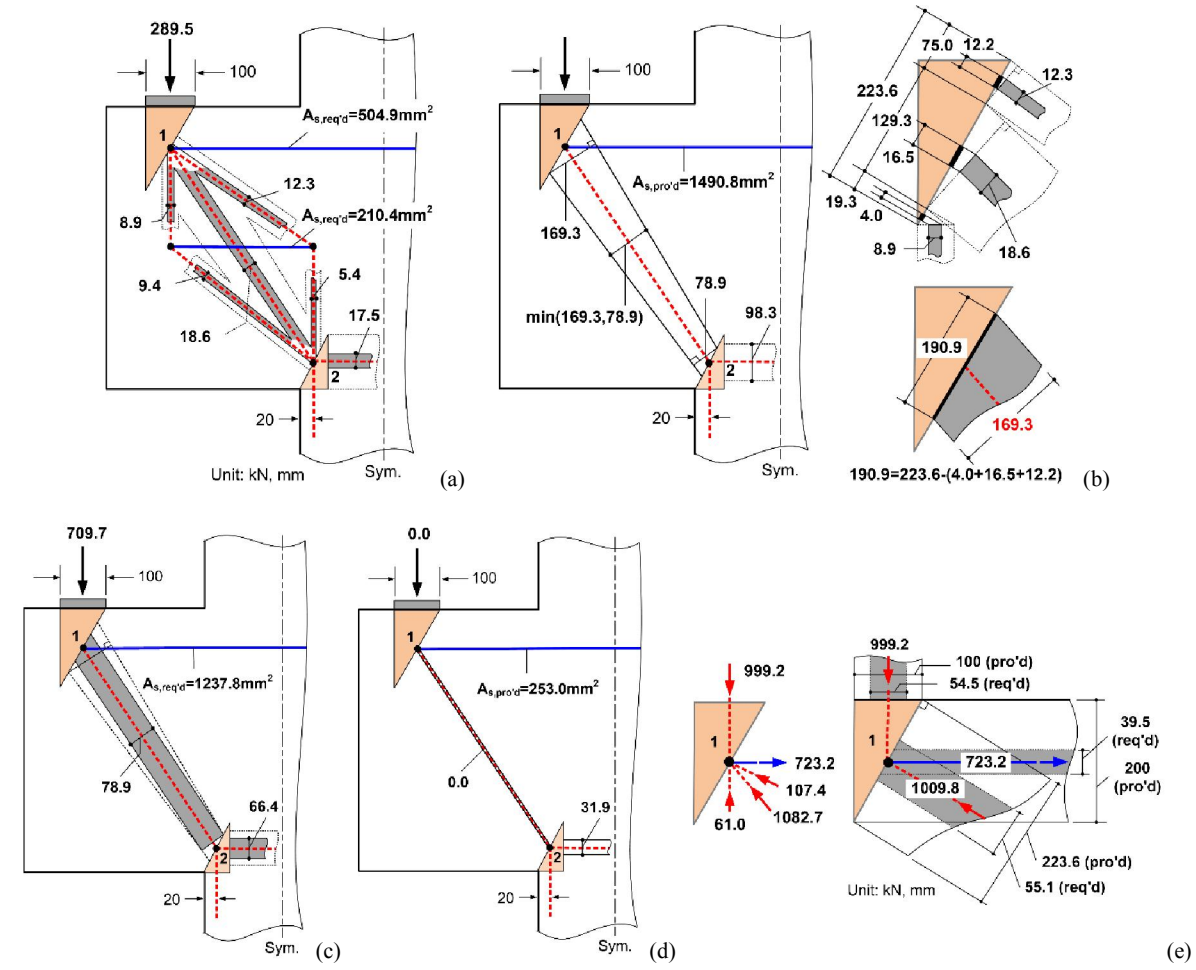

Figure 7. Failure Strength Estimation of Corbel PG2 by an Indeterminate STM. (a) Required Widths/Areas of Struts and Ties at First Failure. (b) Remaining Capacity of Strut and Tie after First Failure. (c) Required Widths/Areas of Struts and Ties at Second Failure. (d) Unstable STM after Second Failure. (e) Strength Verification of CCT Nodal Zone.

Table 5 summarizes the strength analysis results for the 146 corbels. The average ratios of the calculated strength to experimental strength (and COV) by the indeterminate arch mechanism STM with the strut and nodal zone strengths of EC2, DIN, FIB, CSA, ACI 318, and the present study are 0.74 (32.9%), 0.82 (31.1%), 0.65 (36.6%), 0.88 (29.5%), 0.85 (30.5%), and 0.99 (27.0%), respectively. The proposed strut and nodal zone strengths with the indeterminate STM predicted the failure strengths most accurately, implying that the recommended strength values are adequate for corbels' design using the indeterminate STM. The more conservative results by the design codes come from using the lower strengths of struts and nodal zones. The average strength coefficients of the inclined strut D (and CCT nodal zone) in the combined mechanism STM in Figure 5(c) by EC2, DIN, FIB, CSA, ACI 318, and the present study are 0.51(0.72), 0.64(0.64), 0.44(0.61), 0.76(0.76), 0.56(0.69), and 0.86(0.91), respectively. When comparing Tables 3 and 5, the indeterminate STM yields better results than the determinate STMs, indicating that corbels' failure strengths are affected by the type of STM used. Figure 8 compares some of the strength analysis results.

Table 5. Failure Strength Estimated by an Indeterminate STM

P_{cal} / P_{test}

STM Model \ Strut & Node Strength	EC2 [13]	DIN [15]	FIB [1]	CSA [14]	ACI 318 [3]	Present Study
Model (A)	0.67	0.77	0.58	0.82	0.81	0.90
Model (B)	0.77	0.85	0.66	0.91	0.87	1.02
Model (C)	0.79	0.85	0.70	0.91	0.87	1.04
Mean (146)*	0.74	0.82	0.65	0.88	0.85	0.99
COV (%)	32.9	31.1	36.6	29.5	30.5	27.0

(A)~(C): STMs whose horizontal coordinates of node 2 are located at distances of 10%, 15%, and 20% of column width from the left face of the column, respectively; COV: coefficient of variation; ( )*: number of corbels having horizontal shear reinforcing bar(s)

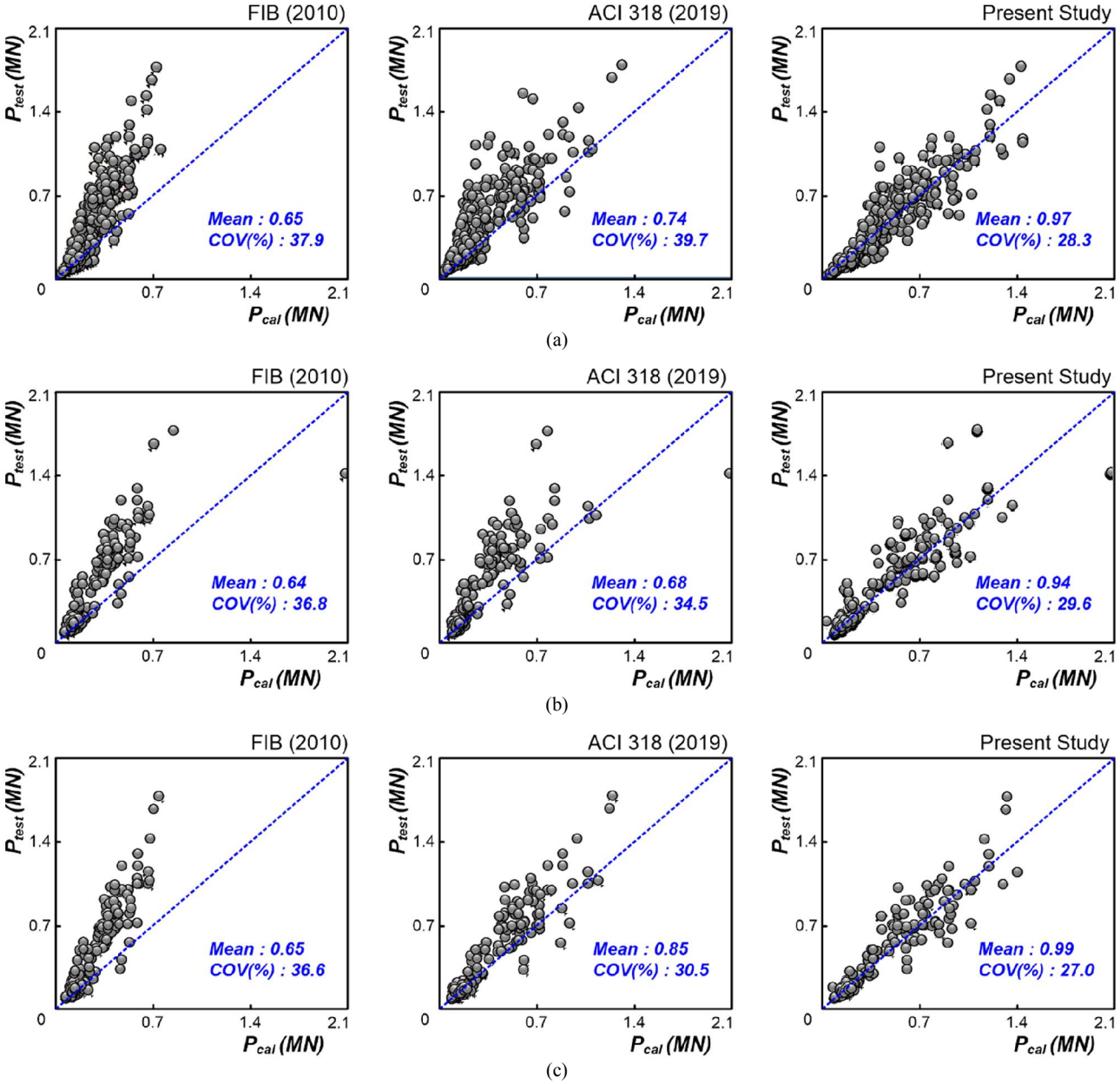

Figure 8. Failure Strengths Estimated by Determinate and Indeterminate STMs. (a) Arch Mechanism. (b) Truss Mechanism. (c) Combined Mechanism

4. Conclusion

For the safe and economical design of RC corbels using the STM methods, designers must accurately determine the strength of concrete struts and nodal zones. In this study, the authors suggested a numerical process for determining the strengths of concrete struts and nodal zones in RC corbels. Besides, for practical application of the recommended process, the authors proposed the strut strength equations that apply to the typical determinate and indeterminate STMs of RC corbels. The authors considered the effects of the primary corbel design variables, including the shear span-to-effective depth ratio, the horizontal-to-vertical load ratio, and the primary tensile and horizontal shear reinforcement ratios in the development of the strength equations. The authors evaluated the validity of the proposed strut and nodal zone strengths by predicting tested 391 RC corbels' failure strengths. In the strength prediction, the authors employed three typical determinate and indeterminate corbel STMs. The average ratios of the calculated strength to experimental strength (and COV) by the strut and nodal zone strengths of EC2, DIN, FIB, CSA, ACI 318, and the present study are 0.74~0.77 (32.9~34.9%), 0.81~0.82 (31.1~32.0%), 0.64~0.65 (36.6~37.9%), 0.70~0.88 (29.5~39.0%), 0.68~0.85 (30.5~39.7%), and 0.94~0.99 (27.0~29.6%), respectively. The failure strengths predicted by the proposed strengths are consistent. They agree reasonably well with experimental results, indicating that the proposed strut and nodal zone strengths can be useful for RC corbels' rational STM design.

5. Declarations

5.1. Author Contributions

Conceptualization, Y.Y.M.; methodology, Y.Y.M.; software, Y.Y.M. and L.Y.J.; validation, Y.Y.M. and L.Y.J.; formal analysis, Y.Y.M.; investigation, Y.Y.M. and L.Y.J.; writing original draft, Y.Y.M.; review and editing, Y.Y.M.; visualization, Y.Y.M. and L.Y.J.; supervision, Y.Y.M.; project administration, Y.Y.M.; funding acquisition, Y.Y.M. All authors have read and agreed to the published version of the manuscript.

5.2. Data Availability Statement

The data presented in this study are available on request from the corresponding author.

5.3. Funding

This research was supported by Basic Science Research Program through the National Research Foundation of Korea (NRF) funded by the Ministry of Education (NRF-2018R1D1A1B06041177).

5.4. Conflicts of Interest

The authors declare no conflict of interest.

6. References

[1] FIB, CEP-FIP Model Code 2010, Comité Euro-International du Bé ton, International Federation for Structural Concrete, Lausanne, Switzerland, (2010). doi:10.1002/9783433604090.

[2] AASHTO, AASHTO LRFD Bridge Design Specifications, 8th Edition, American Association of State Highway and Transportation Officials, Washington DC, (2018).

[3] ACI, Building Code Requirements for Structural Concrete (ACI 318-19) and Commentary (ACI 318R-19), American Concrete Institute, Farmington Hills, MI, 2019. doi:10.14359/51716937.

[4] B. Thulimann, Shear Strength of Reinforced and Prestressed Concrete - CEB Approach, SP 59-6, American Concrete Institute, Farmington Hills, MI, 1976. doi:10.14359/17767.

[5] M. P. Nielsen, M. W. Braestrup, B. C. Jensen, and F. Bach, Concrete Plasticity, Beam Shear - Shear in Joints - Punching Shear, Special Publication, Danish Society for Structural Science and Engineering, Lyngby, Denmark, (1978).

[6] J. A. Ramirez and J. E. Breen, Proposed Design Procedure for Shear and Torsion in Reinforced and Prestressed Concrete, Research Report 248-4F, Center for Transportation Research, University of Texas at Austin, TX, (1983).

[7] P. Marti, "Basic Tools of Reinforced Concrete Beam Design," American Concrete Institute, 82(1), 46-56, 1985. doi:10.14359/10314.

[8] Schlaich, Jorg, Kurt Schafer, and Mattias Jennewein. "Toward a Consistent Design of Structural Concrete." PCI Journal 32, no. 3 (May 1, 1987): 74–150. doi:10.15554/pcij.05011987.74.150.

[9] A. Alshegeir, Analysis and Design of Disturbed Regions with Strut-tie Models, Ph.D. Dissertation, School of Civil Engineering, Purdue University, IN, (1992).

[10] K. Bergmeister, J. E. Breen, J. O. Jirsa, and M. E. Kreger, Detailing in Structural Concrete, Research Report 1127-3F, University of Texas at Austin, TX, (1993).

[11] Yun, Young Mook, and Julio A. Ramirez. "Strength of Struts and Nodes in Strut-Tie Model." Journal of Structural Engineering 122, no. 1 (January 1996): 20–29. doi:10.1061/(asce)0733-9445(1996)122:1(20).

[12] J. G. MacGregor, Reinforced Concrete - Mechanics and Design, 3rd Edition, Prentice Hall, Englewood Cliffs, NJ, (1997).

[13] European Committee for Standardization, Eurocode 2: Design of Concrete Structures, Brussels, Belgium, (2004). doi:10.3403/02214914.

[14] Canadian Standards Association, Design of concrete structures (CSA A23.3-14), Rexdale, ON, Canada, (2014).

[15] Building and Civil Engineering Standards Committee, Plain, Reinforced and Prestressed Concrete Structures - Part 1: Design and Construction (DIN 1045-1), Deutsches Institut Fur Normung E.V., Berlin, (2008).

[16] Yun, Y. M., and J. A. Ramirez. "Strength of Concrete Struts in Three-Dimensional Strut-Tie Models." Journal of Structural Engineering 142, no. 11 (November 2016): 04016117. doi:10.1061/(asce)st.1943-541x.0001584.

[17] ACI Subcommittee 445, Examples for the Design of Structural Concrete with Strut-and-Tie Models, SP-208, American Concrete Institute, Farmington Hills, MI, (2002).

[18] Yun, Young Mook, and Hyun Soo Chae. "An Optimum Indeterminate Strut-and-Tie Model for Reinforced Concrete Corbels." Advances in Structural Engineering 22, no. 12 (May 8, 2019): 2557–2571. doi:10.1177/1369433219845689.

[19] KCI, Examples of Strut-Tie Model Design of Structural Concretes, Kimoondang, Korean Concrete Institute, Seoul, Korea, (2013).

[20] M. P. Collins and D. Mitchell, Prestressed Concrete Structures, Prentice Hall, Englewood Cliffs, NJ, (1997).

[21] E. G. Nawy, Prestressed Concrete: A Fundamental Approach, 5th Edition, Pearson Prentice Hall, Upper Saddle River, NJ, (2009).

[22] J. K. Wight, Reinforced Concrete: Mechanics and Design, 7th Edition, Pearson Prentice Hall, Upper Saddle River, NJ, (2016).

[23] Kriz, L. B., and C. H. Raths. "Connections in Precast Concrete Structures—Strength of Corbels." PCI Journal 10, no. 1 (February 1, 1965): 16–61. doi:10.15554/pcij.02011965.16.61.

[24] B. R. Hermansen and J. Cowan, "Modified Shear-Friction Theory for Bracket Design." ACI Journal Proceedings 71, no. 2 (1974): 55-60. doi:10.14359/11169.

[25] Mattock, Alan H., K. C. Chen, and K. Soongswang. "The Behavior of Reinforced Concrete Corbels." PCI Journal 21, no. 2 (March 1, 1976): 52–77. doi:10.15554/pcij.03011976.52.77.

[26] N. I. Fattuhi and B. P. Hughes, "Ductility of Reinforced Concrete Corbels Containing Either Steel Fibers or Stirrups." ACI Structural Journal 86, no. 6 (1989): 644-651. doi:10.14359/2660.

[27] N. I. Fattuhi and B. P. Hughes, "Reinforced Steel Fiber Concrete Corbels With Various Shear Span-to-Depth Ratios." ACI Materials Journal 86, no. 6 (1989). doi:10.14359/2243.

[28] Yong, Yook - Kong, and P. Balaguru. "Behavior of Reinforced High - Strength - Concrete Corbels." Journal of Structural Engineering 120, no. 4 (April 1994): 1182-1201. doi:10.1061/(asce)0733-9445(1994)120:4(1182).

[29] Fattuhi, N. I. "Strength of SFRC Corbels Subjected to Vertical Load." Journal of Structural Engineering 116, no. 3 (March 1990): 701–718. doi:10.1061/(asce)0733-9445(1990)116:3(701).

[30] N. I. Fattuhi, "Reinforced Corbels Made with Plain and Fibrous Concretes." ACI Structural Journal 91, no. 5 (1994): 530-536. doi:10.14359/4166.

[31] N. I. Fattuhi, "Reinforced Corbels Made With High-Strength Concrete and Various Secondary Reinforcements." ACI Structural Journal 91, no. 4 (1994): 376-383. doi:10.14359/4142

[32] S. J. Foster, R. E. Powell, and H. S. Selim, "Performance of High-Strength Concrete Corbels." ACI Structural Journal 93, no. 5 (1996): 555-563. doi:10.14359/9714.

[33] M. Bourget, Y. Delmas, and F. Toutlemonde, "Experimental Study of the Behavior of Reinforced High-Strength Concrete Short Corbels." Materials and Structures 34, no. 237 (November 8, 2005): 155–162. doi:10.1617/13620.

[34] G. Campione, L. L. Mendola, and M. Papia, "Flexural Behaviour of Concrete Corbels Containing Steel Fibers or Wrapped with FRP Sheets." Materials and Structures 38, no. 280 (January 21, 2005): 617–625. doi:10.1617/14210.

[35] G. Campione, L. L. Mendola, and M. L. Mangiavillano, "Steel Fiber-Reinforced Concrete Corbels: Experimental Behavior and Shear Strength Prediction." ACI Structural Journal 104, no. 5 (2007): 570-579. doi:10.14359/18859.

[36] Yang, Jun-Mo, Joo-Ha Lee, Young-Soo Yoon, William D. Cook, and Denis Mitchell. "Influence of Steel Fibers and Headed Bars on the Serviceability of High-Strength Concrete Corbels." Journal of Structural Engineering 138, no. 1 (January 2012): 123–129. doi:10.1061/(asce)st.1943-541x.0000427.

[37] Urban, Tadeusz, and Łukasz Krawczyk. "Strengthening Corbels Using Post-Installed Threaded Rods." Structural Concrete 18, no. 2 (April 2017): 303–315. doi:10.1002/suco.201500215.

[38] Khosravikia, Farid, Hyun su Kim, Yousun Yi, Heather Wilson, Hossein Yousefpour, Trevor Hrynyk, and Oguzhan Bayrak. "Experimental and Numerical Assessment of Corbels Designed Based on Strut-and-Tie Provisions." Journal of Structural Engineering 144, no. 9 (September 2018): 04018138. doi:10.1061/(asce)st.1943-541x.0002137.

[39] Wilson, Heather R., Hossein Yousefpour, Michael D. Brown, and Oguzhan Bayrak. "Investigation of Corbels Designed According to Strut-and-Tie and Empirical Methods." ACI Structural Journal 115, no. 3 (May 2018). doi:10.14359/51701917.

[40] Abdul-Razzaq, Khattab Saleem, and Asala Asaad Dawood. "Corbel Strut and Tie Modeling – Experimental Verification." Structures 26 (August 2020): 327–339. doi:10.1016/j.istruc.2020.04.021.

[41] Ivanova, Ivelina, Jules Assih, and Dimitar Dontchev. "Influence of Anchorage Length of Composite Fabrics and Bonded Surface on the Strengthened Short Reinforced Concrete Corbel by Bonding CFRF." European Journal of Environmental and Civil Engineering 24, no. 12 (September 27, 2018): 1993–2009. doi:10.1080/19648189.2018.1498395.

[42] A. J. Abdulridha, H. K. Risan, and Z. M. Taki, "Numerical Analysis of Reinforced Concrete Corbel Strengthening by CFRP under Monotonic Loading," International Journal of Civil Engineering and Technology, 9(10), (2018): 1554-1565.

[43] Romanichen, R. M., and R. A. Souza. "Reinforced Concrete Corbels Strengthened with External Prestressing." Revista IBRACON de Estruturas e Materiais 12, no. 4 (August 2019): 812–831. doi:10.1590/s1983-41952019000400006.

[44] F. J., Al-Talqany, and Alhussainy A. M. "Stractural Behavior of Reinforced Concrete Corbel Using High-Strength Materials under Monotonic and Repeated Loads." International Journal of Applied Science 2, no. 2 (April 17, 2019): p1. doi:10.30560/ijas.v2n2p1.

[45] Shakir, Qasim M. "Response of Innovative High Strength Reinforced Concrete Encased-Composite Corbels." Structures 25 (June 2020): 798–809. doi:10.1016/j.istruc.2020.03.056.

[46] ACI-ASCE Subcommittee 445, Further Examples for the Design of Structural Concrete with Strut-and-Tie Models, SP-273, American Concrete Institute, Farmington Hills, MI, (2010).

[47] Lee, Seong-Cheol, Jae-Yeol Cho, and Frank J. Vecchio. "Model for Post-Yield Tension Stiffening and Rebar Rupture in Concrete Members." Engineering Structures 33, no. 5 (May 2011): 1723–1733. doi:10.1016/j.engstruct.2011.02.009.